RSC Advances

PAPER

View Article Online
View Journal | View Issue

Cite this: *RSC Adv.*, 2017, **7**, 27377

A binary polymer composite of graphitic carbon nitride and poly(diphenylbutadiyne) with enhanced visible light photocatalytic activity

Juying Lei,[a] Fenghui Liu,[b] Lingzhi Wang,[b] Yongdi Liu*[a] and Jinlong Zhang*[bc]

Received 27th March 2017
Accepted 18th May 2017

DOI: 10.1039/c7ra03534a

rsc.li/rsc-advances

New polymer composites consisting of poly(diphenylbutadiyne) (PDPB) and g-C_3N_4 have been successfully prepared. UV-vis diffuse reflectance spectra show that the existence of PDPB in composites can clearly increase the visible light absorption of the catalysts. Photoluminescence spectroscopy and photoelectrochemical measurements reveal that PDPB can effectively facilitate the charge carrier separation in the composites. Compared with pure g-C_3N_4 or pure PDPB, the composite catalysts exhibit observably enhanced visible-light photocatalytic activity for degradation of RhB and phenol. A possible mechanism for the charge separation and transfer in the composite catalysts is proposed. In addition, the composite catalysts show stable catalytic performance after five successive runs, displaying potential for applications in various fields of photocatalysis.

Introduction

Using semiconductor photocatalysts to degrade organic pollutants has attracted much attention due to the global energy crisis and environment pollution.[1–3] To date, a variety of environmentally responsible photocatalysts have been developed, including TiO_2,[4–7] ZnO,[8,9] CdS[10,11] and so on. In particular, graphitic carbon nitride (g-C_3N_4), a novel metal-free material with a special layered structure, has unique properties, such that it is considered to be an ideal material for photocatalysis.[12,13] In 2009, Wang *et al.* first reported that g-C_3N_4 has excellent photocatalytic ability.[14] Since then, the catalytic performance of g-C_3N_4 for the photocatalytic degradation of organic pollutants in water has been extensively studied.

However, the g-C_3N_4 has many weak points such as the small surface area, high recombination rate of photogenerated electron–hole pairs and low visible light utilization efficiency.[15] Hence, various methods have been used to solve these problems, for example, synthesizing different structures,[16,17] doping with metal or nonmetal elements,[18–21] coupling with other semiconductors,[22–26] and modifying by conjugated polymers.[27,28] Among these methods, the conjugated polymer modification has attracted many attentions because the conjugated polymer not only can enhance the absorption of the visible light but also can act as a semiconductor. Yan *et al.* synthesized carbon nitride–poly(3-hexylthiophene) (g-C_3N_4–P_3HT) composite photocatalyst.[24] They found that the novel photocatalyst exhibited significantly enhanced photocatalytic activity. Thakare *et al.* reported on the synthesis of a ternary polymer composite of graphene, carbon nitride, and poly(3-hexylthiophene) (G–g-C_3N_4–P_3HT) which had enhanced photocatalytic activity.[29] Ge *et al.* prepared a novel polyaniline–graphitic carbon nitride (PANI/g-C_3N_4) composite photocatalyst which had intensive visible light photocatalytic activity.[30] Wang *et al.* prepared an efficient visible-light photocatalyst using g-C_3N_4 and ordinary polyvinyl chloride (PVC) as main precursors.[28] However, to the best of our knowledge, the report about using polymer modified g-C_3N_4 is still scarce.

Poly(diphenylbutadiyne) (PDPB) is a newly developed polymer semiconductor which was reported by Hynd Remita in 2015.[31] The PDPB obtained by π-stacking of oligomers presents a high photocatalytic activity and long-term stability. Recent research has also shown that the composite of PDPB and semiconductor ZnO exhibited high visible light photocatalytic activity,[32] due to the visible light harvesting of PDPB. Inspired by this, we speculate that if we combine PDPB with g-C_3N_4, based on the good visible light absorption of g-C_3N_4 itself, the combination of g-C_3N_4 and PDPB will bring a better absorption of visible light, leading to a better visible light activity.

Herein, we prepare a polymer composite photocatalyst consisting of g-C_3N_4 and PDPB (CN-PDPB). The photocatalytic activity is investigated by evaluating the photocatalytic degradation of Rhodamine B (RhB) and phenol. The results exhibit that the CN–PDPB has higher photocatalytic activity than pure g-C_3N_4 and PDPB. It is maybe because the existence of PDPB can

[a]*State Environmental Protection Key Laboratory of Environmental Risk Assessment and Control on Chemical Process, School of Resources and Environmental Engineering, East China University of Science and Technology, 130 Meilong Road, Shanghai 200237, P. R. China. E-mail: ydliu@ecust.edu.cn*

[b]*Key Lab for Advanced Materials, Institute of Fine Chemicals, School of Chemistry and Chemical Engineering, East China University of Science and Technology, 130 Meilong Road, Shanghai 200237, P. R. China. E-mail: jlzhang@ecust.edu.cn*

[c]*Suzhou Jukang New Materials Co. Ltd, 558 Fenhu Road, Suzhou, Jiangsu Province 201211, P. R. China*

obviously improve the absorption of g-C_3N_4 in the visible light range. What's more, the interaction between g-C_3N_4 and PDPB improves the separation efficiency of the photo-generated charge carriers. In addition, the composites catalysts show stable catalytic performance after five successive runs.

Experimental

The preparation of photocatalysts

g-C_3N_4 was synthesized by directly heating melamine powder. Melamine powder was put into a covered alumina crucible and heated in a muffle furnace. Firstly, the powder was heated to 500 °C with a heating temperature rate of 2 °C min^{-1} and kept at this temperature for 2 h, then heated to 520 °C within 10 min and kept at this temperature for 2 h. Finally, we obtained a light yellow g-C_3N_4. The product was ground to powder for further usage.

PDPB was synthesized following the previously method published by Hynd Remita.[31]

The composite catalysts of g-C_3N_4 and PDPB were prepared by impregnating g-C_3N_4 (0.5 g) with an ethanol solution of PDPB for a night, and then the solvent was vapored in oil bath at 363 K. The resultant samples were labeled as 50 : x CN–PDPB, where 50 : x was the mass ratio of g-C_3N_4 and PDPB in the above-mentioned process for preparation of CN–PDPB photocatalysts.

Photocatalytic activity test

The photocatalytic activity of the samples was tested by degradation of RhB dyes and phenol at room temperature using a 300 W xenon lamp with AM 1.5 or 420 nm filter as light source. 10 mg of catalyst powder was added to the 50 mL of 10 mg L^{-1} RhB (or phenol) aqueous solution. Before irradiation, the suspensions were continuously stirred for 30 min in the dark in order to reach an adsorption–desorption equilibrium. At given time intervals, aliquots of the irradiated suspension were collected and centrifuged. The RhB was analyzed by the UV-vis spectra at 553 nm and the phenol was analyzed by a HPLC system.

Results and discussion

Morphology and structural properties

To confirm the structure and morphology of the polymer composites, the g-C_3N_4 and the polymer composite 50 : 2 CN–PDPB were observed by TEM. As shown in Fig. 1, both pure g-C_3N_4 and 50 : 2 CN–PDPB display layered structure. Pure g-C_3N_4 (Fig. 1a) exhibits a flat and smooth surface and it became rough after the modification of PDPB (Fig. 1b). It can be seen clearly that the PDPB distributes on the surface of g-C_3N_4. In addition to TEM, other characterizations were also carried out to prove the existence of PDPB in the composite CN–PPDB.

Fig. 2 shows the wide-angle XRD patterns of pure PDPB, pure g-C_3N_4 and CN–PDPB photocatalysts. The peak at 27.7° in the XRD pattern of g-C_3N_4 coming from the interlayer stacking of aromatic segments can be indexed as the (002) planes. Another pattern at 13.1° indexed as (100) planes is due to the in-plane structural packing motif.[5,33,34] From the XRD patterns of CN–PDPB photocatalysts, we can see that the two characteristic

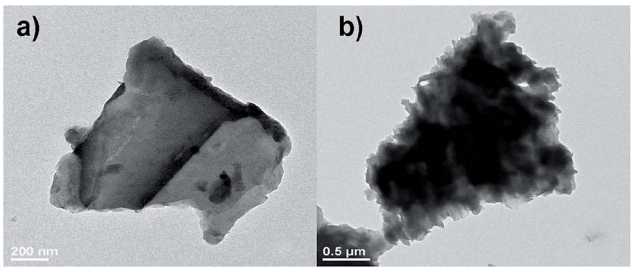

Fig. 1 TEM images of (a) g-C_3N_4 and (b) 50 : 2 CN–PDPB.

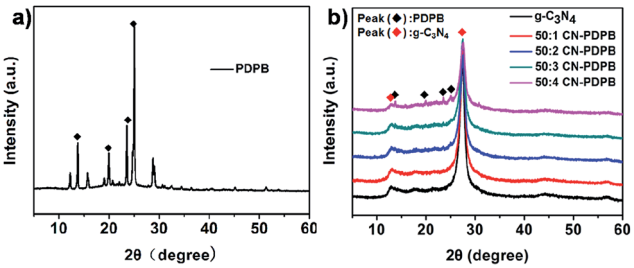

Fig. 2 Wide-angle XRD patterns of (a) PDPB, (b) g-C_3N_4 and CN–PDPB.

peaks of g-C_3N_4 are clearly observed, indicating that PDPB does not change the crystalline structure of g-C_3N_4. However, the characteristic patterns of PDPB are not observed at first because of its low content in the composites but with the increase of content of PDPB, the XRD of 50 : 4 CN–PDPB displays patterns at 14°, 20.4°, 23.6°, 24.7°, which are ascribed to the characteristic patterns of PDPB.[31] This results further confirm the existence of PDPB in the CN–PDPB composites.

The surface chemical environment of the catalysts is analyzed by XPS. Fig. 3a and b show the C 1s XPS spectra of g-C_3N_4 and 50 : 2 CN–PDPB, respectively. In Fig. 3b, the C 1s has two peaks at 284.8 and 288.1 eV. The C peak at 284.8 eV corresponds to graphitic carbon, which is usually observed in the XPS spectrum of carbon nitrides.[35] The peak at 288.1 eV is ascribed to the sp^2-bonded carbon (N–C=N) from carbon nitride and carbon atoms in conjugated structure (–C=C–) from PDPB.[28,36–39] Compared with Fig. 3a, the intensity ratio of the peaks at 284.8 eV and 288.1 eV in Fig. 3b reduces, indicating the existence of –C=C– on the surface of 50 : 2 CN–PDPB. This

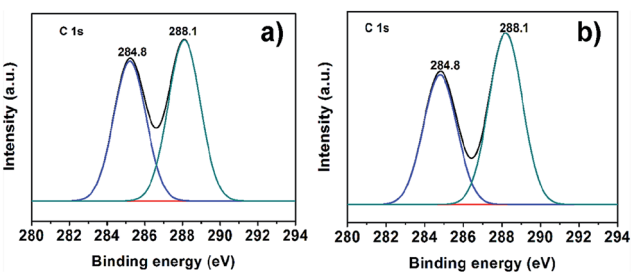

Fig. 3 The XPS spectra of (a) C 1s of g-C_3N_4 and (b) C 1s of 50 : 2 CN–PDPB.

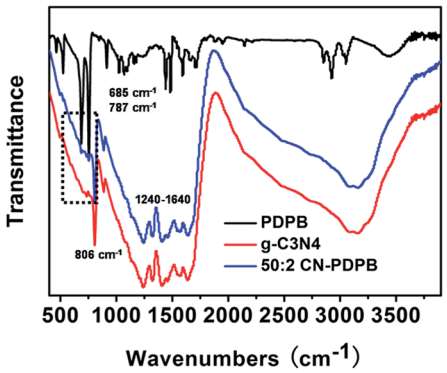

Fig. 4 FTIR spectra of PDPB, g-C_3N_4 and 50 : 2 CN–PDPB.

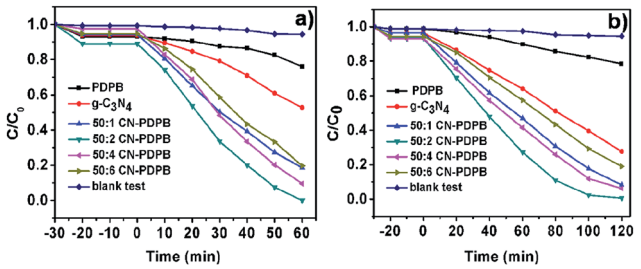

Fig. 6 Photocatalytic degradation of RhB over different catalysts (a) under simulated sunlight (with AM 1.5), (b) under visible light irradiation (λ > 420 nm).

further confirms the existence of PDPB in the composite CN–PDPB.

Fig. 4 shows the FTIR spectra of PDPB, g-C_3N_4 and 50 : 2 CN–PDPB. For g-C_3N_4, the strong bands at 1241, 1322, 1406, 1571, and 1631 cm^{-1} are corresponding to the typical stretching modes of CN heterocycles and the band at 806 cm^{-1} is attributed to the characteristic breathing mode of triazine units. Compared with the FTIR of PDPB and g-C_3N_4, the FTIR band at 685 cm^{-1} and 787 cm^{-1} can be found in 50 : 2 CN–PDPB which is consistence with the previous report[31] but the intensities of the peaks are weak. That is because the low content of PDPB in 50 : 2 CN–PDPB. All of these prove the existence of PDPB in 50 : 2 CN–PDPB.

The UV-vis diffuse reflectance spectrum for the catalysts in Fig. 5 shows that the absorption of the CN–PDPB composites is higher than that of pure g-C_3N_4 in the range of 360–800 nm due to the existence of PDPB. Furthermore, the absorption intensity of the CN–PDPB increases with the increase of PDPB content. This improved absorption is helpful to the improvement of the photocatalytic activity of g-C_3N_4.

Photocatalytic performances

In order to evaluate the photocatalytic activity of the as-synthesized samples, a test reaction is carried out for the degradation of 10 mg L^{-1} of RhB with 10 mg of the catalyst under simulated sunlight or visible light and the results are shown in Fig. 6. In addition, Fig. 7 is the UV-vis spectra of the degraded RhB using the 50 : 2 CN–PDPB under simulated sunlight (with AM 1.5). As can be seen from Fig. 6, no matter under irradiation of simulated sunlight or visible light, the photocatalytic degradation of RhB with the CN–PDPB composites is clearly higher than that of the pure g-C_3N_4 and the pure PDPB. The reason may be ascribed to that the combination of g-C_3N_4 and PDPB can improve the separation efficiency of the photo-generated electrons and holes, meaning the recombination of electrons and holes is inhibited. However, from Fig. 6 we can also find that with the content of PDPB increased, the photocatalytic activity of CN–PDPB composites increases at first and then decreases, and the 50 : 2 CN–PDPB shows the highest photocatalytic activity. This is because with the contents of PDPB increase, extra PDPB will hinder the light exposed to g-C_3N_4 and less g-C_3N_4 can be excited to generate electron–hole pairs. As a result, the catalytic activity is reduced. Therefore, there is an optimal ratio to achieve the best photocatalytic activity.

In addition, we use TOC measurement to further confirm the degree of mineralization of RhB solution. The RhB solution is almost decolorized after 60 min irradiation (in Fig. 6a) and about 30% removal of TOC has been seen in Fig. 8, manifesting that RhB has been not only decolorized but also mineralized partly.

Phenol was chosen as another model pollutant to eliminate the sensitization effect of RhB.[5] Fig. 9 presents the results of

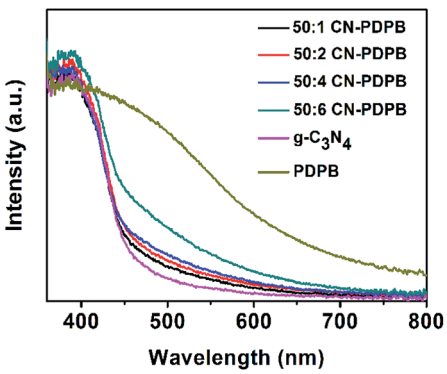

Fig. 5 UV-vis diffuse reflectance spectra of pure g-C_3N_4 and CN–PDPB composites.

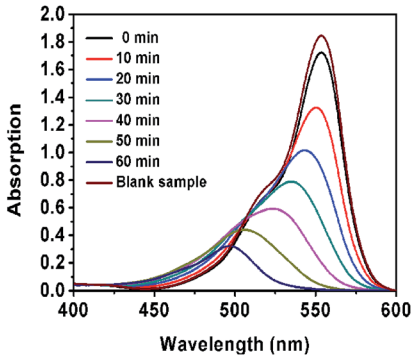

Fig. 7 The UV-vis spectra of the degraded RhB using the 50 : 2 CN–PDPB under simulated sunlight (with AM 1.5).

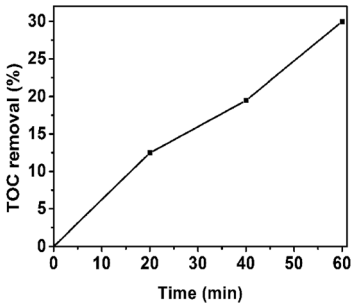

Fig. 8 TOC removal of RhB solution in the presence of 50 : 2 CN–PDPB.

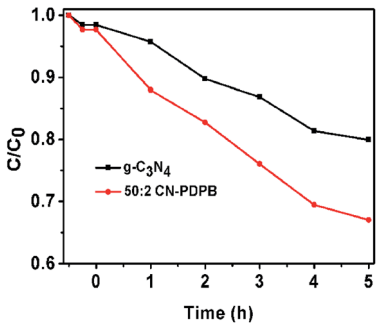

Fig. 9 Photocatalytic degradation of phenol over different catalysts under visible light irradiation.

photocatalytic degradation of phenol catalyzed by pure g-C_3N_4 and 50 : 2 CN–PDPB under visible light irradiation. We can see that the photocatalytic degradation efficiency of phenol with 50 : 2 CN–PDPB is obviously higher than that of pure g-C_3N_4, further illustrating that the composite has increscent photocatalytic activity. In addition, we use TOC measurement to further confirm the degree of mineralization of phenol solution. From Fig. 10, it can be seen that the TOC removal values are increased. The degradation of phenol takes time until being finally mineralized.

Mechanism for the enhanced photocatalytic activity

To investigate the mechanism for the enhancement of the photocatalytic activity by the modification of g-C_3N_4 with PDPB,

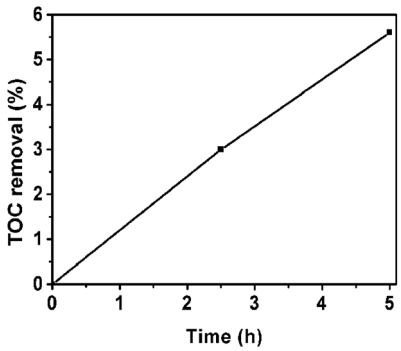

Fig. 10 TOC removal of phenol solution in the presence of 50 : 2 CN–PDPB.

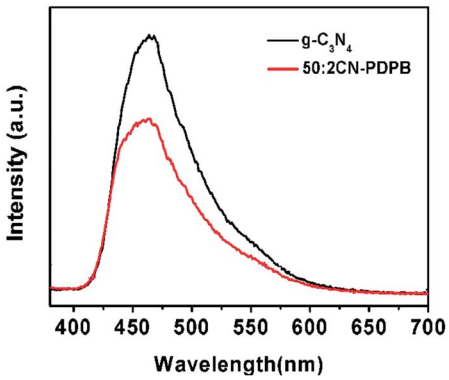

Fig. 11 Photoluminescence spectra of g-C_3N_4 and 50 : 2 CN–PDPB.

photoluminescence (PL) spectra were measured. Fig. 11 shows the results of PL spectra of pure g-C_3N_4 and 50 : 2 CN–PDPB excited at 360 nm. As can be seen from the figure, the pure g-C_3N_4 exhibits a PL emission band at 460 nm. In comparison, the PL intensity of 50 : 2 CN–PDPB composites is lower than that of g-C_3N_4 due to the easy transfer of carriers between g-C_3N_4 and PDPB, indicating the increase in the separation efficiency of photo-generated electron–hole pairs.[40–42]

Besides the photoluminescence measurement, electrochemical impedance spectroscopy (EIS) is also applied to investigate the charge transfer resistance of the catalysts.[43–45] The EIS results of prepared samples are presented in Fig. 12 in the form of Nyquist plots. It can be clearly found that the g-C_3N_4 has the highest charge transport resistance for its biggest arc radius and the arc radius of CN–PDPB is significantly smaller than that of the pure g-C_3N_4. In addition, the 50 : 2 CN–PDPB has the smallest arc radius among the prepared materials, revealing an effective separation of photogenerated electron–hole pairs and faster charge transfer occurred on 50 : 2 CN–PDPB.

To further investigate the photocatalytic mechanism of the CN–PDPB, the transient photocurrent responses of pure g-C_3N_4 and 50 : 2 CN–PDPB were tested by on–off cycles of irradiation.

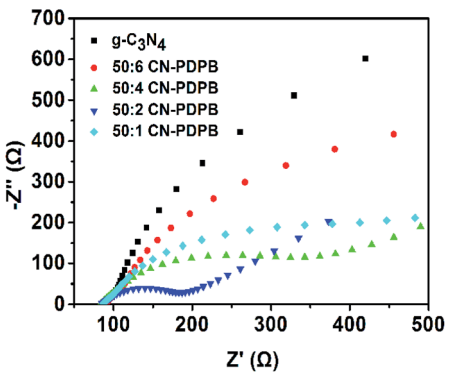

Fig. 12 Electrochemical impedance spectroscopy of g-C_3N_4 and CN–PDPB photocatalysts.

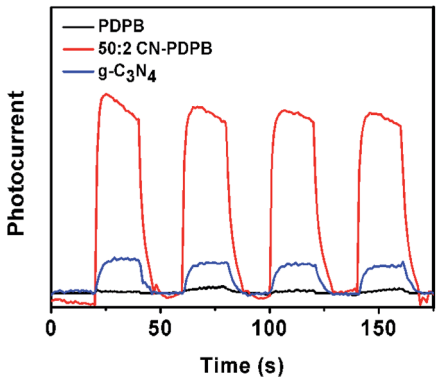

Fig. 13 Transient photocurrent response for PDPB, g-C_3N_4 and 50 : 2 CN–PDPB photocatalysts.

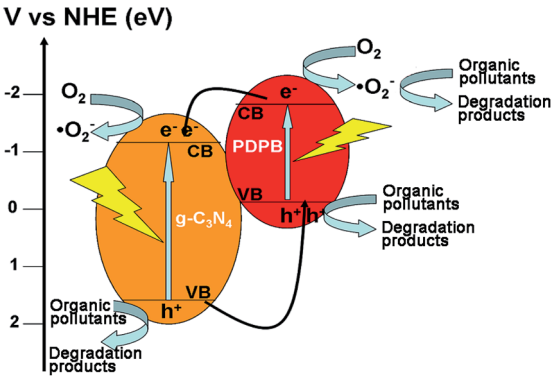

Fig. 15 The proposed photocatalytic mechanism of CN–PDPB composites.

Transient photocurrent analysis is also a widely used typical method to investigate the electron–hole separation effect for a material.[46] In Fig. 13, it can be seen that the photocurrent of 50 : 2 CN–PDPB is much larger than the photocurrent of pure g-C_3N_4, indicating higher separation and transfer efficiency of photo-generated electrons and holes due to the synergetic effect of g-C_3N_4 and PDPB.

The effects of benzoquinone (BQ, a typical $^{\bullet}O_2^-$ scavenger) and disodium oxalate ($Na_2C_2O_4$, a typical hole scavenger) on the photodegradation of RhB in the presence of 50 : 2 CN–PDPB are investigated. From the Fig. 14, we can see that the BQ clearly inhibits the photodegradation of RhB, but the $Na_2C_2O_4$ lightly decreases the photodegradation of RhB, indicating that the $^{\bullet}O_2^-$ and the holes are all effective for the degradation of RhB but the $^{\bullet}O_2^-$ is the main active species for the RhB degradation.

On the basis of the above experiments and results, the mechanism is explained in Fig. 15. With irradiation of light, both g-C_3N_4 and PDPB can be excited to produce photo-generated electrons and holes. The conduction band (CB) position of PDPB (−1.78 eV) is more negative than that of g-C_3N_4 (−1.13 eV), and the valence band (VB) position of g-C_3N_4 (+1.57 eV) is more positive than that of PDPB (+0.18 eV).[31] Hence, the photo-generated electrons of PDPB can easily transfer to the conduction band (CB) of g-C_3N_4, while the holes of g-C_3N_4 can transfer to the valence band (VB) of PDPB. Thus, the recombination of photo-generated electrons and holes can be inhibited and an effective charge separation is achieved, resulting in a remarkable enhancement of the photocatalytic activity. Moreover, the major possible reactions can be displayed as follows:

$$\text{CN–PDPB} + h\nu \rightarrow \text{g-}C_3N_4\text{*–PDPB*}$$

$$\text{g-}C_3N_4\text{*–PDPB*} \rightarrow \text{g-}C_3N_4\ (e^-e^-/h^+h^+)\text{–PDPB}\ (e^-e^-/h^+h^+)$$

$$\text{g-}C_3N_4\ (e^-e^-/h^+h^+)\text{–PDPB}\ (e^-e^-/h^+h^+) \rightarrow \text{g-}C_3N_4\ (e^-e^-e^-/h^+)\text{–PDPB}\ (e^-/h^+h^+h^+)$$

$$e^- + O_2 \rightarrow {}^{\bullet}O_2^-$$

$$^{\bullet}O_2^- + \text{organic pollutants} \rightarrow \text{degradation products}$$

$$h^+ + \text{organic pollutants} \rightarrow \text{degradation products}$$

The stability of photocatalyst is another important issue for a photocatalyst. The recycling runs in the photodegradation of RhB in the presence of 50 : 2 CN–PDPB are carried out. Fig. 16 shows that the photocatalytic degradation degree of RhB still remains high after 5 cycles, manifesting the catalyst has good photocatalytic stability.

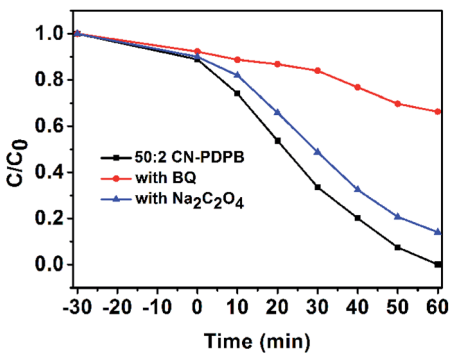

Fig. 14 Effects of BQ and $Na_2C_2O_4$ on RhB photodegradation catalyzed by 50 : 2 CN–PDPB photocatalysts.

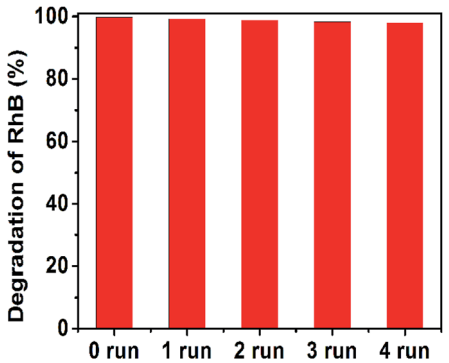

Fig. 16 Effect of cycling runs on RhB degradation in the presence of 50 : 2 CN–PDPB under visible-light irradiation.

Conclusions

In summary, a new photocatalyst has been prepared by compounding g-C_3N_4 and the polymer PDPB *via* a facile method. The photocatalytic activity of CN–PDPB composites is much higher than that of the pure catalysts (g-C_3N_4 or PDPB), which is confirmed by the photocatalytic degradation of RhB and phenol under simulated solar light or visible light. With the increase of PDPB content, the photocatalytic activity increases at first and then decreases, and 50 : 2 CN–PDPB has the highest photocatalytic activity. The enhanced photocatalytic activity may be caused by the increased charge separation which can be attributed to the synergistic effect between g-C_3N_4 and PDPB. In addition, the photocatalytic stability of the catalyst is good. This study is hopeful to provide some experience for the synthesis of other polymer composited g-C_3N_4 or other semiconductor composited PDPB in the application of photocatalysis and other fields.

Acknowledgements

The authors wish to express their deepest and sincerest recognition of Prof. András Dombi a key figure in the topic of photocatalytic materials for the degradation of contaminants of environmental concern. This work was financially supported by National Nature Science Foundation of China (21407049, 21377038, 21237003 and 21677048), China Postdoctoral Science Foundation (2015T80409), Shanghai Pujiang Program (14PJ1402100), the Science and Technology Commission of Shanghai (16JC1401400) and the Science and Technology Commission of Jiangsu Province (BC2015135).

References

1 A. Fujishima and K. Honda, *Nature*, 1972, **238**, 37–38.
2 C. Chen, W. Ma and J. Zhao, *Chem. Soc. Rev.*, 2010, **39**, 4206–4219.
3 S. Dong, J. Feng, M. Fan, Y. Pi, L. Hu, X. Han, M. Liu, J. Sun and J. Sun, *RSC Adv.*, 2015, **5**, 14610–14630.
4 W. Wang, Y. Liu, J. Qu, Y. Chen and Z. Shao, *RSC Adv.*, 2016, **6**, 40923–40931.
5 H. Li, L. Zhou, L. Z. Wang, Y. D. Liu, J. Lei and J. L. Zhang, *Phys. Chem. Chem. Phys.*, 2015, **17**, 17406–17412.
6 H. Li, X. Shen, Y. Liu, L. Wang, J. Lei and J. Zhang, *J. Alloys Compd.*, 2016, **687**, 927–936.
7 M. Nasir, J. Lei, W. Iqbal and J. Zhang, *Appl. Surf. Sci.*, 2016, **364**, 446–454.
8 S. G. Kumar and K. S. R. K. Rao, *RSC Adv.*, 2015, **5**, 3306–3351.
9 Y. Xu, H. Xu, H. Li, J. Xia, C. Liu and L. Liu, *J. Alloys Compd.*, 2011, **509**, 3286–3292.
10 Y. Liu, P. Zhang, B. Z. Tian and J. L. Zhang, *ACS Appl. Mater. Interfaces*, 2015, **7**, 13849–13858.
11 S. Singh and N. Khare, *RSC Adv.*, 2015, **5**, 96562–96572.
12 J. Lei, Y. Chen, F. Shen, L. Wang, Y. Liu and J. Zhang, *J. Alloys Compd.*, 2015, **631**, 328–334.
13 H. Li, L. Wang, Y. Liu, J. Lei and J. Zhang, *Res. Chem. Intermed.*, 2016, **42**, 3979–3998.
14 X. C. Wang, K. Maeda, A. Thomas, K. Takanabe, G. Xin, J. M. Carlsson, K. Domen and M. Antonietti, *Nat. Mater.*, 2009, **8**, 76–82.
15 Z. W. Zhao, Y. J. Sun and F. Dong, *Nanoscale*, 2015, **7**, 15–37.
16 J. Hong, X. Xia, Y. Wang and R. Xu, *J. Mater. Chem.*, 2012, **22**, 15006–15012.
17 Y. Xu, M. Xie, S. Huang, H. Xu, H. Ji, J. Xia, Y. Li and H. Li, *RSC Adv.*, 2015, **5**, 26281–26290.
18 X. F. Chen, J. S. Zhang, X. Z. Fu, M. Antonietti and X. Wang, *J. Am. Chem. Soc.*, 2009, **131**, 11658–11659.
19 L. Zhang, X. Chen, J. Guan, Y. Jiang, T. Hou and X. Mu, *Mater. Res. Bull.*, 2013, **48**, 3485–3491.
20 Y. Zhang, T. Mori, J. Ye and M. Antonietti, *J. Am. Chem. Soc.*, 2010, **132**, 6294–6295.
21 S. C. Yan, Z. S. Li and Z. G. Zou, *Langmuir*, 2010, **26**, 3894–3901.
22 J. Lei, Y. Chen, L. Wang, Y. Liu and J. Zhang, *J. Mater. Sci.*, 2015, **50**(9), 3467–3476.
23 L. Zhou, L. Wang, J. Lei, Y. Liu and J. Zhang, *Catal. Commun.*, 2017, **89**, 125–128.
24 L. Zhou, L. Wang, J. Zhang, J. Lei and Y. Liu, *Eur. J. Inorg. Chem.*, 2016, 5387–5392.
25 Y. S. Xu and W. D. Zhang, *ChemCatChem*, 2013, **5**, 2343–2351.
26 S. Z. Wu and K. Li, *Appl. Surf. Sci.*, 2015, **324**, 324–331.
27 H. J. Yan and Y. Huang, *Chem. Commun.*, 2011, **47**, 4168–4170.
28 D. S. Wang, H. T. Sun, Q. Z. Luo, X. L. Yang and R. Yin, *Appl. Catal., B*, 2014, **156**, 323–330.
29 S. Gawande and S. R. Thakare, *ChemCatChem*, 2012, **4**, 1759–1763.
30 L. Ge, C. C. Han and J. Liu, *J. Mater. Chem.*, 2012, **22**, 11843–11850.
31 S. Ghosh, L. Ramos, S. Remita, A. Dazzi and H. Remita, *Nat. Mater.*, 2015, **14**, 505–511.
32 S. Sardar, P. Kar, H. Remita, B. Liu, P. Lemmens, S. K. Pal and S. Ghosh, *Sci. Rep.*, 2015, **5**, 17313–17326.
33 Y. Xu, M. Xie, S. Huang, H. Xu, H. Ji, J. Xia, Y. Li and H. Li, *RSC Adv.*, 2015, **5**, 26281–26290.
34 Y. Xu, S. Huang, M. Xie, Y. Li, H. Xu, L. Huang, Q. Zhang and H. Li, *RSC Adv.*, 2015, **5**, 95727–95735.
35 X. Jian, X. Liu, H. M. Yang, J. G. Li, X. L. Song, H. Y. Dai and Z. H. Liang, *Appl. Surf. Sci.*, 2016, **370**, 514–521.
36 S. W. Cao, Y. P. Yuan, J. Fang, M. M. Shahjamali, F. Y. C. Boey, J. Barber, S. C. J. Loo and C. Xue, *Int. J. Hydrogen Energy*, 2013, **8**, 1258–1266.
37 L. Ge, C. Han, J. Liu and Y. Li, *Appl. Catal., A*, 2011, **409–410**, 215–222.
38 Y. Wang, X. Wang and M. Antonietti, *Angew. Chem., Int. Ed.*, 2012, **51**, 68–89.
39 A. Vinu, *Adv. Funct. Mater.*, 2008, **18**, 816–827.
40 B. Subash, B. Krishnakumar, M. Swaminathan and M. Shanthi, *Res. Chem. Intermed.*, 2013, **39**, 3181–3197.
41 K. Yadav, M. Giri and N. Jaggi, *Res. Chem. Intermed.*, 2015, **41**, 9967–9978.
42 A. K. L. Sajjad, S. Shamaila, B. Z. Tian, F. Chen and J. L. Zhang, *Appl. Catal., B*, 2009, **91**, 397–405.

43 C. Zeng, M. Guo, B. Tian and J. Zhang, *Chem. Phys. Lett.*, 2013, **575**, 81–85.
44 C. Zeng, B. Tian and J. Zhang, *J. Colloid Interface Sci.*, 2013, **405**, 17–21.
45 X. Liu, L. J. Chen, R. Y. Chen, Z. Chen, X. Chen and X. Zheng, *Res. Chem. Intermed.*, 2015, **41**(6), 3623–3636.
46 K. Dai, L. Lu, Q. Liu, G. Zhu, X. Wei, J. Bai, L. Xuan and H. Wang, *Dalton Trans.*, 2014, **43**, 6295–6299.